

established by methods of X-ray phase analysis and infrared spectroscopy. The maximum saturation magnetization was found for the composition $\text{Mn}_{0.3}\text{Fe}_{2.7}\text{O}_4$ ($M_s = 68 \text{ A} \cdot \text{m}^2 \cdot \text{kg}^{-1}$ at 300 K and $M_s = 85 \text{ A} \cdot \text{m}^2 \cdot \text{kg}^{-1}$ at 5 K), which is associated with a change in the cationic distribution over tetrahedral and octahedral voids. The materials obtained were stabilized in the form of colloidal solutions using a number of polyelectrolytes. It was found that poly(diallyldimethylammonium chloride) – PDDA had the best stabilizing effect due to its structural features. A method for controlling the magnetic properties of magnetite by partial replacement of iron ions in the magnetite structure with manganese is proposed. Changing the magnitude of the magnetization and coercive force is possible by changing the degree of substitution. Relatively high values of specific magnetization, as well as uniformity of magnetic particles in size, can be of practical interest, for the manufacture of contrast agents in MRI diagnostics.

Key words: nanoparticles; saturation magnetization; contrast agents; MRI diagnostics.

Полный текст материалов доклада будет опубликован в журнале «Журнал Белорусского государственного университета. Физика»; 2021 г.

STRUCTURE AND ELECTRONIC PROPERTIES OF $\text{MoS}_{1.5}\text{Se}_{0.5}$ ALLOY FROM FIRST-PRINCIPALS CALCULATIONS

V. Gusakov¹, J. Gusakova², B. Tay³

¹⁾ *Scientific-Practical Materials Research Center of NASB, P. Browki 19, 220072 Minsk, Belarus, e-mail: gusakov@ifftp.bas-net.by*

²⁾ *Novitas Center, Nanyang Technological University, 50 Nanyang Ave. 639798 Singapore, e-mail: julia001@e.ntu.edu.sg*

³⁾ *CINTRA UMI CNRS/NTU/THALES, 50 Nanyang Drive 637553 Singapore, e-mail: ebktay@ntu.edu.sg*

Corresponding author: V. Gusakov (gusakov@ifftp.bas-net.by)

The effects of relative positions of Se atoms in a real monolayer alloy $\text{MoS}_{1.5}\text{Se}_{0.5}$ have been studied. It is demonstrated that the distribution of Se atoms between top and bottom chalcogen planes is most energetically favorable. For a more probable distribution of Se atoms $\text{MoS}_{1.5}\text{Se}_{0.5}$ monolayer alloy is a direct semiconductor with the fundamental band gap equal 2.35 eV. We have also evaluated the optical band gap of alloy at 77 K (1.86 eV) and room temperature (1.80 eV), which is in good agreement with the experimentally measured band gap of 1.79 eV.

Key words: transition metal dichalcogenides; alloy; DFT.

INTRODUCTION

Semiconducting transition metal dichalcogenides (TMDs) represent a class of layered materials with a nonzero band gap, which exploration started decades ago and continues until present [1, 2]. Transition metal dichalcogenides have attracted much attention owing to their rich physics and promising applications in electronic and optoelectronic devices [2]. TMD monolayers such as MoS_2 , MoSe_2 , WS_2 , WSe_2 are direct band gap semiconductors (with optical band gap of 1–2 eV) [3]. The crystal-phase engineering of TMDs is criti-

cally important to form new structures phase-based TMD, showing tunable physicochemical properties.

In this report we present the theoretical analysis of the energy of formation of monolayer $\text{MoS}_{2(1-x)}\text{Se}_{2x}$ alloy ($x = 0.25$) and the microscopic structural stability (different alloy configurations with variation of positions of substituting atoms of Se). Our study is based on the recently proposed GVJ-2e method, developed within DFT framework for accurate band gap calculation [4, 5, 6, 7].

RESULTS

$\text{MoS}_{2(1-x)}\text{Se}_{2x}$ alloy represents 2D monolayer alloy. It is built from MoS_2 monolayer, when some of S atoms are substituted with Se atoms. We considered $\text{MoS}_{2(1-x)}\text{Se}_{2x}$ alloy with substitution rate of S equal to 25% ($x=0.25$).

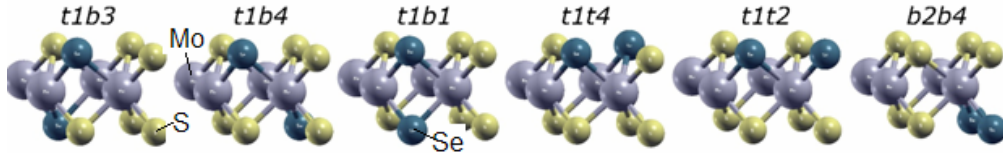


Figure 1. – $\text{MoS}_{1.5}\text{Se}_{0.5}$ monolayer alloy with different Se atoms positions

Thus two Se atoms substituted two S atoms in MoS_2 supercell containing 12 atoms. There are several possible atomic positions for the Se atoms. Such configurations include the distribution of Se atoms between top and bottom chalcogen planes (t1b3, t1b4, ‘stacking’ t1b1) and occupation of a single chalcogen plane by Se atoms (t1t2, t1t4, b2b4). Fig. 1 demonstrates all configurations t1b1, t1b3, t1b4, t1t2, t1t4, b2b4 of MoS_2 monolayer with two S atoms substituted with Se which corresponds to $\text{MoS}_{1.5}\text{Se}_{0.5}$ alloy. We analyzed the formation energy of $\text{MoS}_{1.5}\text{Se}_{0.5}$ supercell with different positions of Se atoms to study the real structure of alloy. The formation energy ($E_{\text{formation}}$) of the particular configuration of alloy is calculated according to

$$E_{\text{formation}} = E_{\text{MoS}_{2(1-x)}\text{Se}_{2x}} - (1-x)E_{\text{MoS}_2} - xE_{\text{MoSe}_2} \quad (1)$$

where E is the total energy of the supercell. The t1b3 and t1b4 configurations have the lowest formation energy. The t1b1 configuration (stacking of Se atoms on top of each other) has higher formation energy but still negative. The configurations in which both Se atoms are located at the same plane (t1t4, t1t2, b2b4) have positive formation energy. The latter makes them less likely to appear during the synthesis of $\text{MoS}_{1.5}\text{Se}_{0.5}$ alloy.

We calculate the fundamental band gaps of $\text{MoS}_{1.5}\text{Se}_{0.5}$ alloy with different positions of Se atoms using GVJ-2e method. Table presents calculated GVJ-2e fundamental band gap of $\text{MoS}_{1.5}\text{Se}_{0.5}$ alloy.

Table

Theoretical fundamental band gap (GVJ-2e) of MoS_2 , MoSe_2 , $\text{MoS}_{1.5}\text{Se}_{0.5}$ (for each configuration) monolayers. Experimental band gaps - STS measurement. All values are in eV

1L	MoS_2	MoSe_2	$\text{MoS}_{1.5}\text{Se}_{0.5}$						
			t1b3	t1b4	t1b1	t1t4	t1t2	b2b4	$\text{MoS}_{1.5}\text{Se}_{0.5}$
GVJ-2e	2.38	2.12	2.37	2.37	2.34	2.33	2.33	2.32	<2.35>
Exp.	2.40 [7]	2.18 [9]	—	—	—	—	—	—	—

The value of the fundamental band gap not only depends on the substitution rate but is also sensitive to relative positions of Se atoms in MoS_2 matrix. The average value of the fundamental band gap lies between experimental values of 2.40 eV, 2.5 eV for MoS_2 , and 2.18 eV for MoSe_2 [7, 8, 9] and corresponds to about 30 % shift from experimental band gap of monolayer MoS_2 towards MoSe_2 .

We provide the calculation of the fundamental band gap, which should be compared with an experimentally obtained band gap via scanning tunneling spectroscopy (STS) measurement. Usually from experiment the optical band gap is available (determined from photoluminescence spectrum (PL)). It was shown previously [10, 11] that the $\text{MoS}_{2(1-x)}\text{Se}_{2x}$ alloy band gap are mostly in the red part of a visible spectrum (1.65–2.0 eV). PBE calculations [12] give the value of $\text{MoS}_{1.5}\text{Se}_{0.5}$ band gap 1.63 eV, which differs from the experimentally obtained value of 1.79 eV by 0.16 eV (9%). So we also estimate optical band gap ($E_g(\text{PL})$) for $\text{MoS}_{1.5}\text{Se}_{0.5}$ alloy at low temperature ($E_g(\text{PL}) = E_g(\text{QP}) - E(\text{exc. binding})$). The theoretical exciton binding energy ($E(\text{exc. binding})$) has been calculated on the basis of BSE (Bethe–Salpeter equation) theory and equals to 0.501 eV and 0.465 eV for MoS_2 and MoSe_2 monolayers respectively [13]. The exciton binding energy in alloy $\text{MoS}_{1.5}\text{Se}_{0.5}$ was obtained by interpolating the exciton binding energy of MoS_2 and MoSe_2 monolayers and was equal 0.492 eV. Thus for $\text{MoS}_{1.5}\text{Se}_{0.5}$ alloy configurations optical band gap at low temperature ranges from 1.83 to 1.88 eV. The estimated optical gap at room temperature of 1.80 eV agrees well with experimental value 1.79 eV [14] (deviation of 0.01 eV).

We have analyzed electronic band structure and the projected densities of states of $\text{MoS}_{1.5}\text{Se}_{0.5}$ alloy in comparison with MoS_2 and MoSe_2 . The calculation shows that $\text{MoS}_{1.5}\text{Se}_{0.5}$ monolayer alloy is a direct band gap semiconductor similarly to the monolayers of MoS_2 and MoSe_2 (see Fig. 2).

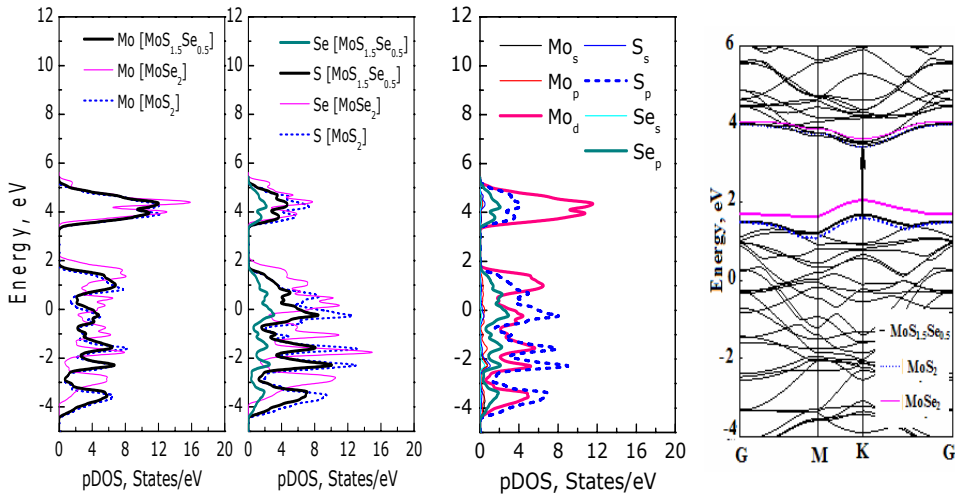


Figure 2. – Band diagram of $\text{MoS}_{1.5}\text{Se}_{0.5}$ alloy (t1b3) with top v-band and bottom c-band lines of MoS_2 and MoSe_2 (LDA PZ)

The presence of Se atoms in MoS₂ matrix affects not only pDOS of sulphur but also pDOS of molybdenum. Presence of Se atoms shifts and changes the shape of Mo pDOS (and the number of states/eV) in the compound comparing to monolayer MoS_{1.5}Se_{0.5} alloy pDOS is dominated by Mo_d, S_p and Se_p states.

We have also analyzed the electron effective mass for the alloy ($0 < x < 1$). Practically for the whole region of substitution rate the electron effective mass is smaller than the free electron mass. It should be also noted that for the substitution rate in the range $0.6 < x_S < 0.9$ ($0.1 < x_{Se} < 0.4$) some peculiarity is observed (electrons become heavier than holes), but more detailed calculations are needed. We have obtained the following effective masses in MoS₂ monolayer: $m_e^* = 0.33m_0$ and $m_h^* = 0.40m_0 \mu_{exc}^{direct}$ ($=18m_0$) and in MoSe₂ are $m_e^* = 0.42m_0$ and $m_h^* = 0.49m_0 \mu_{exc}^{direct}$ ($=23m_0$) from Kohn-Sham band structure calculated using PBE GGA. Also in our calculations for MoS₂ and MoSe₂ monolayers both electrons and holes have effective masses smaller than a free electron mass, which agrees well with results obtained with G₀W₀ and HSE [15, 16]. Comparison of the effective masses of electrons (holes) in the alloy with the effective masses of electrons in MoS₂ and MoSe₂ monolayers reveals that electrons (holes) become slightly heavier in the alloy.

CONCLUSIONS

The first principles calculations of the structure and electronic properties (fundamental and optical band gap) of 2D alloy MoS_{1.5}Se_{0.5} have been presented. Analysis of the formation energies of the MoS_{1.5}Se_{0.5} monolayer alloy with different positions of Se atoms shows that alloy configurations with Se atoms distributed between top and bottom chalcogen planes tend to be more energetically favorable during the synthesis. The calculation shows that MoS_{1.5}Se_{0.5} monolayer alloy is a direct band gap semiconductor with the fundamental band gap equals to 2.35 eV. We have evaluated the exciton binding energy (0.492 eV) and calculated optical band gaps of MoS_{1.5}Se_{0.5} alloy at low (1.86 eV) and room (1.80 eV) temperatures. The estimated optical gap at room temperature of 1.80 eV agrees well with experimental value 1.79 eV (deviation of 0.01 eV). This fact confirms that experimentally observed PL transitions correspond to an optical band gap. This study also confirms the efficiency of the recently proposed GVJ-2e method for band gap calculations for 2D alloys.

REFERENCES

1. Novoselov, K. S. Two-dimensional atomic crystals / S. Novoselov, D. Jiang, F. Schedin, T. J. Booth, V. V. Khotkevich, S. V. Morozov, A. K. Geim. // Proc. Nat. Acad. Sci. USA – 2005. – Vol. 102, №30. – P. 10451–10453.
2. Tan Ch. Recent Advances in Ultrathin Two-Dimensional Nanomaterials / Ch. Tan, X. Cao, X.-J. Wu, Q. He, J. Yang, X. Zhang, J. Chen, W. Zhao, S. Han, G.-H. Nam, M. Sindoro, H. Zhang. // Chem. Rev. – 2017. – Vol. 117, № 9. – P. 6225–6331.
3. Li X. Graphene and related two-dimensional materials: Structure-property relationships for electronics and optoelectronics / X. Li, L. Tao, Z. Chen, H. Fang, X. Li, X. Wang, J.-B. Xu, and H. Zhu // Appl. Phys. Rev. – 2017. – Vol. 4. – 021306.
4. Efficient DFT method for calculating band-gap and deep levels in semiconductors / J. Gusakova, V. Gusakov // Book of Abstracts 28th International Conference on Defects in Semiconductors (ICDS 2015), Helsinki, Finland, July 27 – 31, 2015.
5. Gusakova J. General approach for band gap calculation of semiconductors and insulators / J. Gusakova, B. K. Tay, V. Gusakov // Phys. Status Solidi A. – 2016. – Vol. 213, №11. – P. 2834–2837.

6. Gusakova J. Electronic Properties of Bulk and Monolayer TMDs: Theoretical Study Within DFT Framework (GVJ-2e Method) / J. Gusakova, X. Wang, L. L. Shiao, A. Krivosheeva, V. Shaposhnikov, V. Borisenko, V. Gusakov, B. K. Tay // *Phys. Status Solidi A*. – 2017. – Vol. 214. – 1700218.
7. Gusakov Vasilii. A New Approach for Calculating the Band Gap of Semiconductors within the Density Functional Method / Vasilii Gusakov // *Solid State Phenomena*. – 2016. – Vol. 242. – P. 434–439.
8. Huang Y. L. Bandgap tenability at single-layer molybdenum disulphide grain boundaries / Y. L. Huang, Y. Chen, W. Zhang, S. Y. Quek, C.-H. Chen, L.-J. Li, W.-T.Hsu, W.-H. Chang, Y. J. Zheng, W. Chen, A. T. S. Wee // *Nat. Commun.* – 2015. – Vol. 6, –6298.
9. Klots A. R. Probing excitonic states in suspended two-dimensional semiconductors by photocurrent spectroscopy / A. R. Klots, A. K. M. Newaz, Bin Wang, D. Prasai, H. Krzyzanowska, J. Lin, D. Caudel, N. J. Ghimire, J. Yan, B. . L. Ivanov, K. A. Velizhanin, A. Burger, D. G. Mandrus, N. H. Tolk, S. T. Pantelides, K. I. Bolotin. *Sci. Rep.* – 2014. – Vol.4. –6608.
10. Ugeda M. M. Giant bandgap renormalization and excitonic effects in a monolayer transition metal dichalcogenide semiconductor / M. M. Ugeda, A. J. Bradley, S.-F. Shi, F. H. da Jornada, Y. Zhang, D. Y. Qiu, W. Ruan, S.-K. Mo, Z. Hussain, Z.-X. Shen, F. Wang, S. G. Louie, M. F. Crommie // *Nat. Mater.* – 2014. – Vol. 13. – 1091.
11. Komsa H.-P. Two-Dimensional Transition Metal Dichalcogenide Alloys: Stability and Electronic Properties / H.-P. Komsa, A. V. Krashenninnikov // *J. Phys. Chem. Lett.* – 2012. – Vol.3, № 23, – P. 3652–3656.
12. Rajbanshi B. The electronic and optical properties of $\text{MoS}_{2(1-x)}\text{Se}_{2x}$ and $\text{MoS}_{2(1-x)}\text{Te}_{2x}$ monolayers / B. Rajbanshi, S. Sarkar, P. Sarkar // *Phys. Chem. Chem. Phys.* – 2015. – Vol.17, №39. –P. 26166–26174.
13. Olsen T. Simple Screened Hydrogen Model of Excitons in Two-Dimensional Materials / T. Olsen, S. Latini, F. Rasmussen, K. S. Thygesen. // *Phys. Rev. Lett.* – 2016. – Vol. 116. – 056401.
14. Feng Q. Growth of Large-Area 2D $\text{MoS}_{2(1-x)}\text{Se}_{2x}$ Semiconductor Alloys / Q. Feng , Y. Zhu , J. Hong , M. Zhang , W. Duan , N. Mao , J. Wu , H. Xu, F. Dong, F. Lin, C. Jin, C. Wang, J. Zhang, L. Xie // *Adv. Mater.* – 2014. – Vol. 26. – P. 2648–2653.
15. Rasmussen Filip A. Computational 2D Materials Database: Electronic Structure of Transition-Metal Dichalcogenides and Oxides / Filip A. Rasmussen, Kristian S. Thygesen // *J. Phys. Chem.* – 2015. – Vol. C 119, №23. – P. 13169–13183.
16. Peelaers H. Effects of strain on band structure and effective masses in MoS_2 / H. Peelaers, C. G. Van de Walle // *Phys. Rev. B*. – 2012. – Vol. 86, № 24. – 241401(R).

NUMERICAL MODELING OF GEOMETRICAL EFFECTS ON MANIPULATION OF EXCHANGE INTERACTION FOR TWO-ELECTRON STATES IN NANOGATES-DONORS SYSTEM

E. A. Levchuk, L. F. Makarenko

Belarusian State University, Nezavisimosti av. 4, 220030 Minsk, Belarus

Corresponding author: E. A. Levchuk (Liauchuk@bsu.by)

Numerical simulation results of exchange coupling in the system of near-surface donor and quantum dot pairs are presented. Exchange energy under the effect of external electric field has been calculated using Hartree-Fock method. Fourier transform and finite element methods have been used to solve the problem for the Poisson equation. The dependences of exchange energy on external electric field have been obtained. Limits of applicability of electric field for the system control are discussed. The effect of donors position has been investigated.

Key words: qubit; two-electron system; nanogate; quantum dot; modeling.